Simulation of Beneficial Compressive Residual Stress Fields as Design Tool in Manufacturing Internally Pressurized Parts

H. Brünnet and D. Bähre

Saarland University, Institute of Production Engineering, Campus A4.2, 66123 Saarbrücken

Abstract: Internally pressurized steel parts, such as components of fuel injection systems, are often treated with manufacturing processes which selectively induce beneficial compressive residual stresses. An available manufacturing technology to do so is hydraulic Autofrettage (AF). With the help of a single over-pressurization, the compressive residual stress field is established right at the most failure critical area of the components, e.g. around the bore in a thick-walled cylinder or at the bore intersection in a pressure distributor block. This allows for the full exploitation of the material potential and the successful implementation of lightweight design concepts. However, the simulation of the material behavior during the process is a difficult task, as anisotropy effects like the Bauschinger effect lead to complex stress-strain relations. This paper presents several approaches to model the material behavior and the corresponding residual stress generation during AF for two representative geometries. The elastic-plastic material behavior is described with different available plasticity formulations in Abaqus/CAE. Additionally, different 2D, 3D and axis-symmetric modeling approaches are compared and the performance of the chosen element types is discussed. Finally, two ways of modeling material removal after AF are presented (implicit = Abaqus/Standard and explicit = Abaqus/Explicit) and suggestions are made to consider the existing interactions along the manufacturing process chain.

Keywords: Residual Stress, Autofrettage, Material Removal, Abaqus/CAE

1. Introduction

Residual stresses are gaining increasing importance in the manufacturing of internally pressurized high performance components, such as components of diesel injection systems. They have to withstand pulsating pressure loads for 250,000 km and more in case of passenger cars or even more than 1,000,000 km in case of heavy duty truck applications. In order to increase the fatigue strength, compressive residual stresses are used as design tool especially in failure critical areas of the components, e.g. the bore wall or bore intersections. The compressive residual stresses superimpose with the later applied load stresses and shift the resulting mean stresses in the compressive area. As a consequence, the fatigue strength is effectively increased [Buxbaum 1983]. Often applied manufacturing processes are shot peening [Kloos, 1987], deep rolling [Scholtes, 1990] or swaging [Gibson, 2008]. However, those manufacturing processes often suffer from restricted access to the relevant internal geometries that have to be treated. Hydraulic Autofrettage (AF) is a manufacturing process that makes use of a pressurized low viscosity hydraulic medium capable of reaching all relevant internal geometries [Bähre, 2011]. It selectively induces compressive residual stresses at the most failure critical areas, making the process very effective.

Following manufacturing processes such as finishing with reaming or honing to achieve the desired form and dimension tolerance, take away a part of the residual stress loaded areas. This leads to redistribution effects and additionally new residual stresses are induced by the finishing process itself, which may be beneficial but also detrimental [Brünnet, 2011].

Therefore, it is important to model the residual stress propagation along the manufacturing process chain in order to evaluate the final residual stress state. Finite element analysis (FEA) is a powerful tool to do so. In this paper, recent advances in the modeling of the AF process and a following boring and reaming operation are presented. Different 2D, 3D and axis-symmetric modeling approaches are compared and available element types are tested with respect to accuracy and calculation time. In addition, rather simple plasticity models are applied and compared to model the material behavior during the AF process accurately but manageable in terms of avoiding complex subroutines for the material description. For verification, the calculated residual stress profiles are compared to different analytical solutions. Finally, two ways of modeling material removal after AF are presented with Abaqus/Standard as well as Abaqus/Explicit and suggestions are made to consider the existing interactions along the manufacturing process chain.

2. Material behavior during AF

AF is known since the early 1900s and was first applied by the French army in order to increase the firing strength of gun barrels [Gibson, 2008]. Nowadays, it is mostly applied in the automotive industry for components of fuel injection systems such as the common rail diesel injection system [Lechmann, 2008]. Other application areas are pressure vessels in the chemical industry, petrochemical industry, and nuclear industry as well as in numerous hydraulic high pressure components. The process principle is fairly simple and explained for the example of a thick-walled cylinder. The cylinder is filled with a hydraulic low viscosity medium and metallically sealed. A pressure intensifier driven by a hydraulic power pack in the AF machine increases the medium pressure well above the yield strength of the treated component. This leads to a partially plastic deformation depending on the applied AF pressure. The rest of the material is elastically deformed. After pressure release, this elastically deformed region tries to relax to its base state but is prevented to do so by the plastically deformed region. Figure 1 illustrates the process schematically.

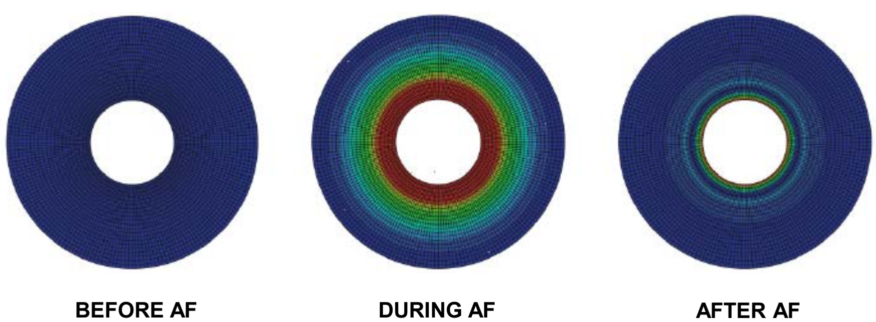

Figure 1. Schematic von Mises equivalent stress development during AF.

As a consequence, a characteristic compressive residual stress profile is induced around the bore and present over several millimeters along the wall thickness. The material behavior during AF can be explained with the help of a stress-strain curve acquired with a uniaxial tension-compression test. Figure 2 defines the relevant regions in the stress-strain curve and introduces the later discussed approximations of the material model.

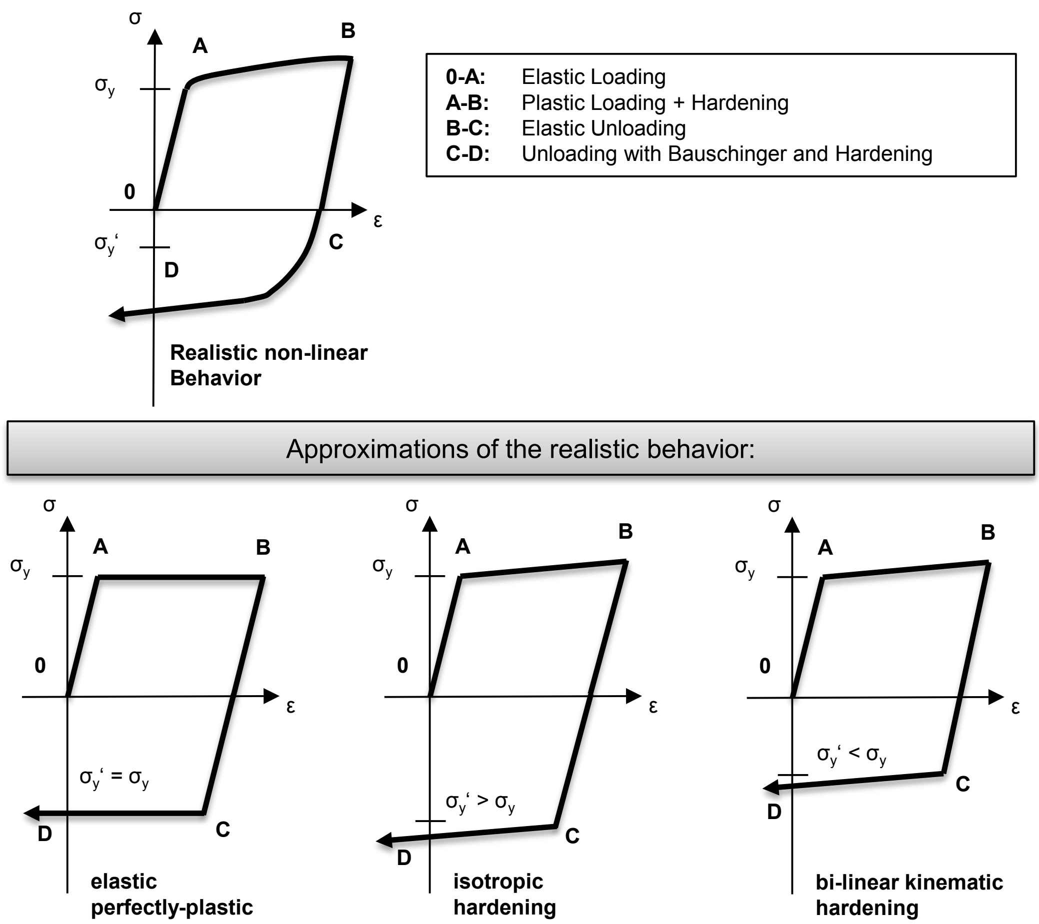

Figure 2. Considered material approximations for stresses and strains during AF.

In the pressure ramp-up phase (0-A), the material follows first an elastic behavior described with Hooke's law. After passing the initial yield strength (σ_y), strain hardening occurs up to the peak AF pressure (A-B). This pressure is hold for some seconds and released afterwards. Here, the material behaves elastic until the yield strength in compression (σ_y') has been reached (B-C). Due to the Bauschinger effect, σ_y' is smaller than σ_y and leads to an early halt of the elastic unloading behavior. Afterwards, strain hardening occurs again until the pressure is zero (C-D). Depending on the wall thickness of the component, another effect can be observed: reverse yielding (re-yielding). The stresses at the bore generated by the elastic recovery become so high, that the material starts to flow in the opposite direction. In addition with the Bauschinger effect, this effectively reduces the amount of inducible compressive residual stresses around the bore. Consequently, it has to be considered when modeling the AF process.

Several analytical approaches have been presented in literature. Seeger et al. [Seeger, 1993] give an analytical solution based on equations presented by Hencky and considering elastic, perfectly-plastic material behavior with the von Mises failure criterion, plane strain and incompressibility of the material in the elastic and plastic regime. The American Society of Mechanical Engineers (ASME) [ASME, 2010] gives design suggestions for pressurized vessels with AF in their "Boiler and Pressure Vessel Code". Their solution considers the Bauschinger effect based on empirically acquired material data from uniaxial tension-compression tests. As the considered materials show a significant Bauschinger effect [O'Hara, 2001], this solution is rather conservative and may over-estimate the material anisotropy. Furthermore, Huang [Huang, 2005] gives a powerful solution to calculate all residual stress components by graphically fitting empirical stress-strain curves from uniaxial tension-compression tests. It is capable to consider all possible material responses including non-linear strain hardening in loading and unloading. The behavior is then described with six parameters. All three approaches are applied in the following investigation.

However, the material behavior has to be implemented in Abaqus. Thumser [Thumser, 2009] uses an approach that makes use of a superposition procedure. Loading and unloading are treated separately. They describe the stress-strain curve alternatively by defining the plastic strain as temperature and making the material temperature depending such that it fits the stress-strain curve. The Abaqus-code is presented along with the results. However, it is not suitable for non-proportional loading distributions, e.g. residual stresses from machining and consecutive AF. Hence, the manufacturing history cannot be considered. Lechmann [Lechmann, 2008] uses the AFC-model of Armstrong, Frederick and Chaboche [Lemaitre, 2009] and corresponding user-dependent material data in the Abaqus subroutine UMAT. This approach is very accurate but requires high experimental effort as the Bauschinger effect is depending on the prior tensile load. O'Hara and Troiano [O'Hara] already compared different simple plasticity models including elastic, perfectly-plastic material behavior and isotropic hardening as well as a bi-linear kinematic hardening approach in Abaqus in order to describe the Bauschinger effect principally. Their approach will be applied and the results are compared to Huang's analytical solution.

3. Convergence study for different AF models in Abaqus/CAE

At the beginning of the process modeling, a convergence study is performed. The thick-walled cylinder is the easiest geometry to model AF due to its axis-symmetry and has the advantage that nearly all relevant 2D and 3D stress elements can be tested with it. In the following convergence study, 2D-elements, 3D-elements and axis-symmetric elements are compared to each other with respect to calculation accuracy and time. For the easiest way of comparison with analytical solutions, the elastic, perfectly-plastic material model is applied. The used PC equipment was a

DELL Precision T1500 with an i7-quad core processer (type 870) with 2.93 GHz and 8 MB memory running on Windows 7 Professional 64 bit. The Abaqus release was 6.10 EF1.

3.1 Geometry, material and process data

The thick-walled cylinder is modeled with an outer diameter (OD) of 27 mm and an inner diameter of 9 mm, i.e. an outer to inner diameter ratio K = 3. Plane strain is used as boundary condition in all models. Therefore, the length of the cylinder is not relevant at this point. All cylinders were treated with an AF pressure of 8,000 bar. The material data was acquired with an uniaxial tensile test following DIN EN 10002 and is presented in Table 1.

Table 1. Material data and geometry of the thick-walled cylinder.

Material data AISI 4140	
Young's modulus	E = 211,000 MPa
Poisson ratio	μ = 0.49999
Yield strength (initial)	σ_y = 973 MPa
Yield strength (compression)	σ_y' = -827 MPa
Ultimate strength	σ_m = 1,073 MPa
Bauschinger effect factor	BEF = $\lvert\sigma_y'\rvert/\lvert\sigma_y\rvert$ = 0.85

3.2 Convergence study 2D model

In 2D, a quarter model is sufficient to model the whole cylinder. The model and the relevant boundary conditions are presented in Figure 3.

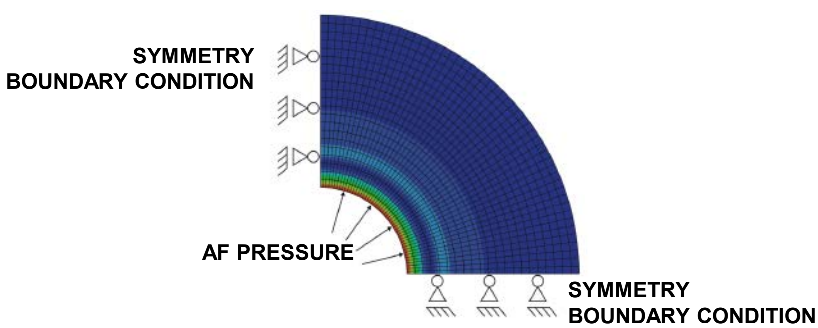

Figure 3. 2D quarter model.

Abaqus/CAE offers different element types to model plane strain in 2D. Here, the following quadratic elements were used:

- CPE4: linear interpolation with 4 nodes.
- CPE4R: linear interpolation with 4 nodes and reduced integration.
- CPE8: second order interpolation with 8 nodes.
- CPE8R: second order interpolation with 8 nodes and reduced integration.

For the mesh control setting, the structured meshing for quad elements was applied. For the AF pressure of 8,000 bar, the maximum hoop stress at the ID of the cylinder was compared to the analytical solution described in [Seeger, 1993]. Table 2 shows the results of the convergence study for a different number of elements.

Table 2. Results of the convergence study for the 2D model.

2D shape	Mesh type	Number of elements	Calculation time [s]	Hoop stress FEA (S22) [MPa]	Analytical calculated hoop stress [MPa]	Percent error [%]
Quarter	CPE4	1500	2021	-681	-677	0.59
	CPE4R	3000	65118	-682	-677	0.74
	CPE8	1500	1986	-681	-677	0.59
	CPE8R	200	62	-684	-677	1.03

The results show a minimum error of 0.59 % for the CPE4 and CPE8 elements but rather high calculation times. CPE4R needs already 18 hours to yield a converged solution. CPE8R converges very fast and yields an acceptable error of approx. 1 %. In principal, all four tested elements are suitable for the AF modeling. With respect to calculation time, CPE8R is favorable.

3.3 Convergence study axis-symmetric model

In 3D, the axis-symmetric model is a powerful and fast solution for the thick-walled cylinder. The model and the relevant boundary conditions are presented in Figure 4.

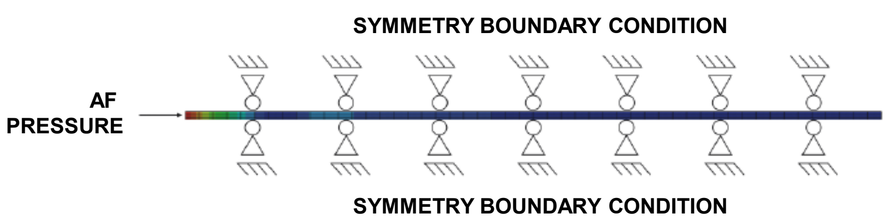

Figure 4. Thin 3D axis-symmetric model of the thick-walled cylinder.

Abaqus/CAE offers different element types to model 3D axis-symmetry. Here, the following quadratic elements were used:

- CAX4: linear interpolation with 4 nodes.
- CAX4R: linear interpolation with 4 nodes and reduced integration.
- CAX8: second order interpolation with 8 nodes.
- CAX8R: second order interpolation with 8 nodes and reduced integration.

For the mesh control setting, the structured meshing for quad elements was applied. For the AF pressure of 8,000 bar, the maximum hoop stress at the ID of the cylinder was compared to the analytical solution described in [Seeger, 1993]. Table 3 shows the results of the convergence study for a different number of elements.

Table 3. Results of the convergence study for the axis-symmetric model.

3D shape	Mesh type	Number of elements	Calculation time [s]	Hoop stress FEA (S22) [MPa]	Analytical calculated hoop stress [MPa]	Percent error [%]
Axial	CAX4	3000	40	-683	-677	0.89
	CAX4R	3000	35	-683	-677	0.89
	CAX8	50000	792	-692	-677	1.92
	CAX8R	100	19	-684	-677	1.03

The results show a minimum error of 0.89 % for the CAX4 and CAX4R elements within reasonable calculation times. The higher order CAX8R element converges very fast and yields an acceptable error of approx. 1 %. Even though the CAX8 element yields an acceptable error of around 2 %, this solution is not converged after nearly 800 s and using 50,000 elements. The final value does change randomly when increasing or decreasing the number of elements. In the case of 100 elements, such as shown with the CAX8R element, the error is as high as 10 %. Therefore, this element cannot be suggested here. Instead, CAX4R or CAX8R should be used.

3.4 Convergence study 3D model

In 3D, a quarter model is sufficient to model the whole cylinder. The length of the cylinder was set to 1 mm, which results in a thin slice. Due to the plane strain boundary condition, this dimension does not affect the calculation results. This 3D convergence study is most important as a lot of real components treated with AF show complex geometries, e.g. bore intersections. Therefore, mainly 3D models and their accompanying elements have to be applied in order to model those geometries. Due to the complexity in 3D, not only the total number of elements is used as parameter but also the element distribution over the corresponding geometry region. Figure 5 introduces the chosen partitions (numbers in circles) that were used to define the different regions and consequently to minimize the total number of elements.

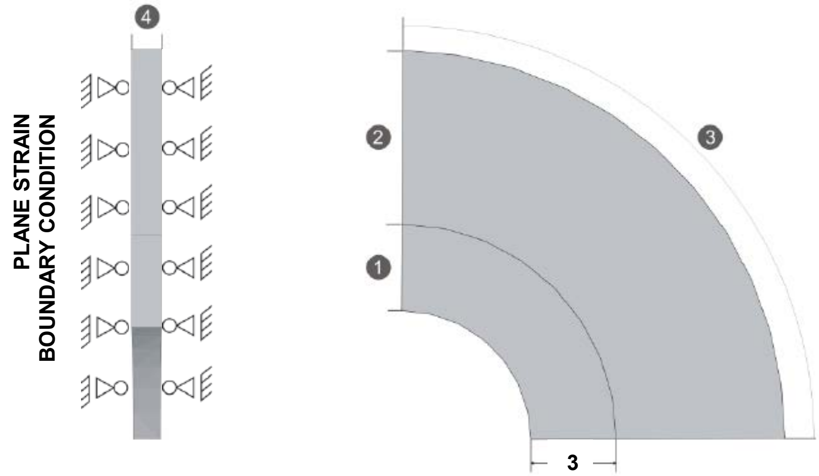

Figure 5. 3D quarter model with partition regions and considered length.

Abaqus/CAE offers different 3D element types. Here, the following elements were used:

- C3D8R: quadratic, linear interpolation with 8 nodes and reduced integration.
- C3D20R: quadratic, second order interpolation with 20 nodes and reduced integration.
- C3D10: tetrahedral, second order interpolation with 10 nodes.
- C3D10H: tetrahedral, second order interpolation with 10 nodes and hybrid formulation.

For the mesh control setting, the structured meshing with a minimization in the mesh transition was applied in case of the quad meshes and the sweep option was applied in case of the tetrahedral meshes. For the AF pressure of 8,000 bar, the maximum hoop stress at the ID of the cylinder was compared to the analytical solution described in [Seeger, 1993]. Table 4 shows the results of the convergence study for a different number of elements with the partition according to Figure 5.

Table 4. Results of the convergence study for the 3D model.

3D shape	Mesh type	Element partition				Calculation time [s]	Hoop stress FEA (S22) [MPa]	Analytical calculated hoop stress [MPa]	Percent error [%]
		1	2	3	4				
Quarter	C3D8R	40	10	20	2	39	-680	-677	0.44
	C3D20R	10	10	50	2	129	-684	-677	1.03
	C3D10	30	10	50	4	383	-684	-677	1.03
	C3D10H	40	10	50	4	621	-684	-677	1.03

The results show a minimum error of 0.44 % for the C3D8R element within fast calculation times. The higher order C3D20R element converges reasonably fast and yields an acceptable error of approx. 1 %. Normally, tetrahedral elements are considered to be critical with respect to their accuracy. In this case, both tested elements C3D10 and C3D10H are suitable even though they consume comparable high calculation times. The crucial point about tetrahedral elements is the superior implementation for complex geometries like sharp bore intersections or tool edges.

3.5 Comparison of the residual stress depth profiles

Not only the amount of compressive stress at the bore is important, but also the depth profile. Therefore, the depth profiles of the converged 2D, 3D and axis-symmetric calculations were compared to each other by means of the residual hoop stresses for the elastic, perfectly-plastic material model at 8,000 bar AF pressure. Additionally, Huang's analytical approach and the ASME approach were used for comparison. This is shown in Figure 6a. Then, different material models were used to approximate the real material behavior during AF as already explained in Figure 2. Three simple approximations were applied in Abaqus/CAE: (1) elastic, perfectly-plastic; (2) elastic, plastic with isotropic hardening; and (3) elastic, plastic with bi-linear kinematic hardening. The residual hoop stress depth profiles were calculated for an AF pressure of 8,000 bar and 11,000 bar. The used element type was CAX4R and the Poisson ratio was set to 0.3. Figure 6b shows the calculated depth profiles.

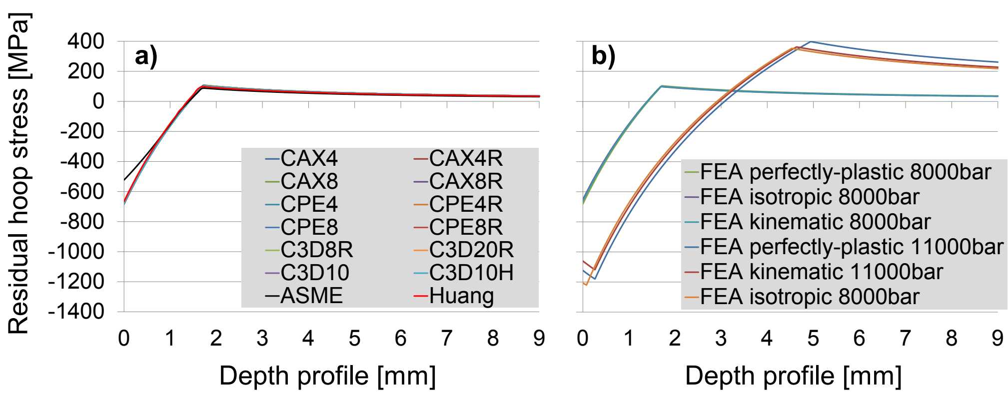

Figure 6. Hoop stress depth profiles for: a) the converged FEA solutions; and b) for different plasticity models at 8,000 and 11,000 bar AF-pressure.

The converged FEA solutions in Figure 6a do not show significant differences with respect to the depth profiles. Actually, the graphs superimpose each other. However, the ASME code yields significant smaller compressive hoop stresses at the bore compared to the FEA and Huang's model. As described by [O'Hara, 2001], the reason is the underlying material data base which consists of materials subjected to high BEF's. Elastic, perfectly-plastic material models will overestimate the compressive hoop stresses. This finding is emphasized when looking at

Figure 6b. The same is true for the elastic, plastic material model with isotropic hardening. As it is not capable of considering the Bauschinger effect, it will overestimate the compressive hoop stresses. This totally agrees with the results found by [O'Hara, 2001]. The elastic, plastic model with bi-linear kinematic hardening shows smaller values right at the bore and significant re-yielding for the 11,000 bar pressure level (re-yielding is also present for the elastic, perfectly-plastic material model). After passing a critical AF pressure, this re-yielding effectively reduces the inducible amount of compressive stresses around the bore. Table 5 presents the input file listings in Abaqus to describe the material.

Table 5. Used material input file listings in Abaqus/CAE.

Elastic, perfectly-plastic	Elastic, plastic with isotropic hardening	Elastic, plastic with kinematic hardening
Material, name=AISI4140* ***Elastic 211000., 0.3** ***Plastic** **973.,0.0**	***Material, name=***AISI4140* ***Elastic 211000., 0.3** ***Plastic** **973.,0.** **1024.,0.0100** **1092.,0.0292** **1124.,0.0435**	***Material, name=***AISI4140* ***Elastic 211000., 0.3** ***Plastic, hardening=KINEMATIC** **973.,0.** **1124.,0.0435**

For more realistic approximations, tensile-compressive stress-strain data needs to be acquired. With this data, the combined hardening approach in Abaqus/CAE can be calibrated and used to (eventually) calculate more accurate compressive stresses. However, for process chain approaches where complex interactions between different manufacturing processes need to be analyzed, the use of the elastic, plastic material model with bi-linear kinematic hardening seems to be a sufficient first approximation covering Bauschinger effect and re-yielding.

4. Application example: high pressure distributor block

In case of a complex geometry like a pressure distributor block with an internal T-shaped bore intersection, it is important to apply a 3D model with appropriate elements. The sharp bore intersection makes the use of solely quadratic elements nearly impossible, therefore tetrahedral elements are used to better fit this geometry. In this application example, C3D10 elements are used. The symmetry of the component is fully exploited, leading to a quarter representation. The mesh was refined manually around the bores and the bore intersection. With the help of this locally refined mesh, the total number of elements can be held down in order to improve the calculation time. However, the calculation still takes around 8 hours for the applied 253,853 elements. The stresses are evaluated along the bisectrix, as this is the most failure critical area and the distribution of the compressive residual stresses is most important for the improvement of the fatigue strength. More details and further results are discussed in [Brünnet, 2011]. Figure 7 shows the residual hoop stress depth profiles after AF with 10,000 bar as well as a cross-sectional view and the Abaqus 3D-model with the corresponding mesh.

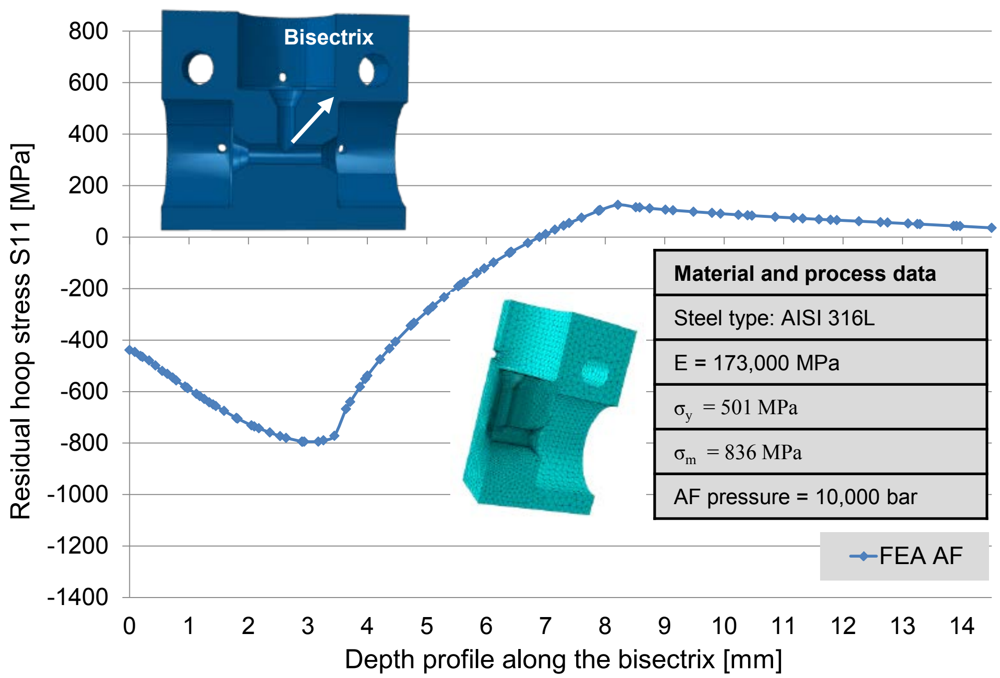

Figure 7. 3D model of a pressure distributor block.

In case of this ductile austenitic stainless steel, pronounced compressive residual hoop stresses can be observed. Re-yielding is also present leading to a significant shift of the maximum compressive hoop stress inside the component.

5. Material removal strategies

Material removal after AF affects the final residual stress distribution as well as the form accuracy of the machined parts due to macroscopic shape deviations caused thereby. Two effects have to be considered when modeling this material removal: first, the redistribution and second, the additional introduction of residual stresses by the machining operation itself. In [Brünnet, 2011] it could be shown that the solely consideration of the redistribution (by simply deleting the relevant elements) will lead to wrong results especially in the surface near region of the machined bores. Therefore, the interaction between tool and work piece is a crucial element of the modeling. The presented results showed a good agreement to residual stress measurements made with a x-ray diffractometer. However, in this paper the focus is more on the implementation of the two material removal strategies in Abaqus/CAE.

5.1 Material removal with "*Model Change, Remove"

The relevant command formulation was implemented directly in the input file. First, the material region that needs to be deleted has to be identified. This can be done by creating a cell partition in the part module. After meshing, the elements in this partition will be selected and a set is created in the assembly module that identifies the relevant elements. If the name of this element set is "Elset", the following two input lines need to be inserted in the prior generated input file at the end of the appropriate "static, general" step for the Abaqus/Standard solver (e.g. material removal):

```
*Model Change, Remove
Elset,
```

Afterwards, the calculation can only be run when a new job is created based on this manually manipulated input file. This leads to the disadvantage that no restart files can be created and used. However, as shown in [Brünnet, 2011] the redistribution is calculated very reliable. Fortunately, the latest release of Abaqus/CAE includes this option directly.

5.2 Material removal with "Progressive damage and failure"

In order to consider the interaction between tool and work piece, an explicit modeling approach has to be used. One promising approach with Abaqus/Explicit is "Progressive damage and failure" [Abaqus, 2012] for ductile metals. It consists of two basic components: first, the damage initiation and second, the damage evolution. However, the objective was not to develop a sophisticated model for machining with chip formation but instead an approximation of the mechanical behavior during the machining. Temperature is considered to be negligible low which is true for finishing operations such as honing. In the first approximation this is also considered for the investigated boring and reaming operation in a stainless steel AISI 316L. For the considered thick-walled cylinder, an AF pressure of 6,350 bar was applied. This was done in a "static, general" step in Abaqus/Standard. Afterwards, the boring and reaming operation was modeled in a second model. Here, the AF material state was imported in the initial step via a pre-defined field. Then, a "dynamic, explicit" step was created for the boring, tool change and reaming operation. The 3D-model is shown in Figure 8, the considered parameters are shown in Figure 9.

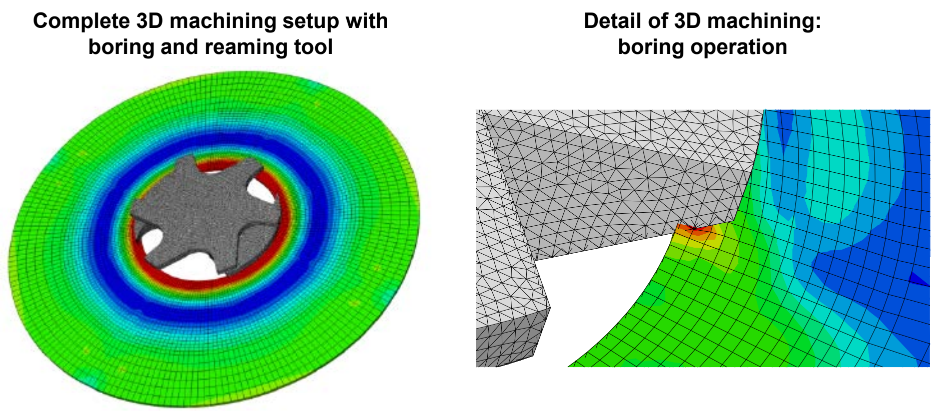

Figure 8. Abaqus/CAE model for boring and reaming.

Simulation step	Parameters	Abaqus/CAE information
AF Abaqus/Standard	AF-pressure: 10,000 bar Density: 8 kg / dm³ Young's modulus: 173,000 MPa Poisson ratio: 0.3 Yield stress: 501 MPa	Boundary condition: plane strain Element type: C3D8R
Boring Abaqus/Explicit	Feed: 19.46 mm / s RPM: 1222.95 1 / s Acceleration factor: 24 Simulation time: 0.026 s Fracture strain: 0.32 Stress triaxiality: 0.33 (tension)	Boundary condition: - OD fixed at four points - Velocity/angular V3 / VR3 Tool: rigid body Initial state: pre-defined field Interaction: general contact
Tool change Abaqus/Explicit	Acceleration factor: 24 Simulation time: 0.0001 s Movement: 0.85 mm	Boundary condition: - OD fixed at four points
Reaming Abaqus/Explicit	Feed: 25.44 mm / s RPM: 799.22 / s Acceleration factor: 24 Simulation time: 0.013 s Fracture strain: 0.32 Stress triaxiality: 0.33 (tension)	Boundary condition: - OD fixed at four points Velocity/angular V3 / VR3 Tool: rigid body Interaction: general contact

Figure 9. Modeling parameters for the Abaqus/EXPLICIT approach.

One crucial point of the simulation is the contact between tool and work piece. It is hard to define an exact border line between elements that are to be removed and elements that will create the new part surface after the machining operation. Additionally, the position of this virtual border line changes due to the priory applied AF pressure and the corresponding plastic deformation. Therefore, appropriate elements sets have to be defined including all possible elements that might have a free surface after the material removal.

Overall, the results presented in [Brünnet, 2011] show that this modeling approach is promising. Further investigations and improvements will be done in the near future including the consideration of temperature-dependent material information and further criteria for the stress triaxiality which mainly defines the damage initiation and therefore the element deletion.

6. Summary and Conclusions

This paper delivers a small insight in the application of Abaqus/CAE for the modeling of the manufacturing process Autofrettage (AF). With the help of a convergence study performed at an axis-symmetric thick-walled cylinder, different 2D, 3D and axis-symmetric stress-strain elements were tested and evaluated with respect to their accuracy and calculation time. The presented results can be used to choose an appropriate element type depending on the complexity of the modeled geometry. Furthermore, three simple plasticity models were compared to different analytical solutions. The elastic, plastic material model with bi-linear kinematic hardening turned out to be the most adequate one as it delivers a first approximation of the Bauschinger effect. Perfect plasticity and isotropic hardening models will overestimate the compressive hoop stresses and are therefore a non-conservative approach to the real material behavior. Clearly, if amount and depth profile need to be calculated as close to reality as possible, more effort has to be spent in the material characterization with uniaxial tension-compression stress-strain tests. Some of those highly sophisticated solutions have been mentioned in the second chapter. However, if the focus lies on the complex interactions along the process chain of Autofrettaged parts, the approximation with the bi-linear kinematic hardening approach is a fast and acceptable solution. The presented results for the material removal after AF emphasize this finding. The input file option "*Model Change, Remove" in Abaqus/CAE does only deliver the redistribution effects when deleting elements. It is not capable of considering the interaction between tool and work piece. The interaction between tool and work piece can be achieved by using the "Progressive damage and failure" option in Abaqus/Explicit. However, it has to be carefully adjusted with adequate material data to consider different damage initiation mechanisms and temperature dependence.

This will be the objective of future investigations.

7. References

1. Abaqus User Manual, Version 6.10-EF1, Dassault Systémes Simulia Corp., Providence, RI.
2. ASME, "Boiler and Pressure Vessel Code – Section VIII, Division 3: Alternative Rules for Construction of High Pressure Vessels, Article KD-5," 2010.
3. Bähre, D., and H. Brünnet, "Modeling of Autofrettage-induced Deformations When Manufacturing High Pressure Parts," Proceedings of NAMRI/SME, 39, TP11PUB24, 2011.

4. Brünnet, H., I. Yi, and D. Bähre, “Modeling of Residual Stresses and Shape Deviations Along the Process Chain of Autofrettaged Components,” Journal of Materials Science and Engineering A, 1/7A, pp. 915-936, 2011.
5. Buxbaum, O., and H. Lowak, “About the Fatigue Strength Improvement Due to Compressive Residual Stresses Induced by Coldworking,” Z. Werkstofftechn., 14, pp. 421-428, 1983.
6. Gibson, M.C., “Determination of Residual Stress Distributions in Autofrettaged Thick-Walled Cylinders,” PhD Theses, Cranfield University, UK, 2008.
7. Huang, X.P., “A General Autofrettage Model of a Thick-Walled Cylinder Based on Tensile-Compressive Stress-Strain Curve of a Material,” J. Strain Analysis, 40/6, pp. 599-607, 2005.
8. Lechmann, M., “Development of a Fatigue Fracture Design Concept for Internal Pressure Loaded Parts With Extensive Compressive Stress Fields,” PhD Thesis, Stuttgart University, Germany, 2008.
9. Lemaitre, J., and J.-L. Chaboche, “Mechanics of Solid Materials,” Cambridge University Press, 2009.
10. Kloos, K.H., and E. Macherauch, “Development of Mechanical Surface Strengthening Processes from the Beginning Until Today,” in: Wohlfahrt, H., R. Kopp, and O. Vöhringer, “Shot Peening – Science, Technology, Application;” DGM, Oberursel, 1987.
11. O’Hara, G.P., and E. Troaino, “Comparison of Autofrettage Calculation Methods,” US Army Techn. Report ARCCB-TR-01001, Watervliet, N.Y., 2001.
12. Scholtes, B., “Eigenspannungen in mechanisch randschicht-verformten Werkstoffzuständen,” pp. 272-294, DGM, Oberursel, 1990.
13. Seeger, T., M. Schön, J.W. Bergmann, and M. Vormwald, “Autofrettage I – Dauerfestigkeitssteigerung durch Autofrettage,” Forschungsvereinigung Verbrennungskraftmaschinen e.V., 1993.
14. Thumser, R., “Simulation des Rissfortschritts in autofrettierten und nicht autofrettierten Bohrungsverschneidungen auf der Grundlage der linear-elastischen Bruchmechanik,” PhD Thesis, Bauhaus University Weimar, Germany, 2009.